Article:
Ham-Karim, HA, Ebili, HO, Manger, K et al. (4 more authors) (2019) Targeted Next-Generation Sequencing Validates the Use of Diagnostic Biopsies as a Suitable Alternative to Resection Material for Mutation Screening in Colorectal Cancer. Molecular Diagnosis & Therapy, 23 (3). pp. 383-393. ISSN 1177-1062

https://doi.org/10.1007/s40291-019-00388-z

Authors: Hersh A. Ham-Karim[1, 2], Henry Okuchukwu Ebili[1, 3], Kirsty Manger[4], Wakkas Fadhil[1], Narmeen S. Ahmad[5, 6], Susan D. Richman[7] and Mohammad Ilyas[1].

Title: Targeted next generation sequencing validates the use of diagnostic biopsies as a suitable alternative to resection material for mutation screening in colorectal cancer.

Affiliations: [1]Division of Pathology, University of Nottingham, Queen's Medical Centre, UK. [2]Department of Medical Laboratory Sciences, College of Health Sciences, Komar University of Science and Technology, Chaq-Chaq-Qualaraisi, Sulaimani City, Iraq. [3]Department of Morbid Anatomy and Histopathology, Olabisi Onabanjo University, Ago-Iwoye, Nigeria. [4]Centre for Medical Genetics, Nottingham University Hospitals NHS Trust, City Hospital Campus, UK. [5]Clinical Oncology, University of Nottingham, City Hospital Campus, UK. [6]Kurdistan Institution for Strategic Studies and Scientific Research, Qirga, Sulaimani, KRG, Iraqi. [7]Department of Pathology and Tumour Biology, Leeds Institute of Cancer and Pathology, Wellcome Trust Brenner Building, St James University Hospital, Leeds, UK

Corresponding author: Dr Henry O. Ebili, University of Nottingham, School of Medicine, Division of Pathology, Queen's Medical Centre, Nottingham, NG7 2UH. Henry.Ebili@nottingham.ac.uk

Key points:

- The findings from this study have lent credence to the growing notion that diagnostic biopsies are very similar to resection samples at the molecular level.
- As such diagnostic biopsies can be used for molecular testing in place of resection samples.
- This creates an opportunity for neoadjuvant therapy and enhances personalised medicine.

ABSTRACT

Background

Mutation testing in the context of neoadjuvant therapy mustbe performed on biopsy samples. Given the issue of tumour heterogeneity, this raises the question of whether the biopsies are representative of the whole tumour. Here we have compared the mutation profiles of colorectal biopsies with their matched resection specimens.

Methods

We performed next generation sequencing (NGS) analysis on 25 paired formalin-fixed, paraffin-embedded (FFPE) colorectal cancer (CRC) biopsy and primary resection samples. DNA was extracted and analysed using the Trusight tumour kit, allowing the interrogation of 26 cancer driver genes. Samples were run on an Illumina MiSeq. Mutations were validated using quick-multiplex-consensus (QMC)-PCR in conjunction with High Resolution Melting (HRM). The paired biopsy and resection tumour samples were assessed for presence or absence of mutations, mutant allele frequency ratios, and allelic imbalance status.

Results

A total of 81 mutations were detected, in 10 of the 26 genes in the Trusight Kit. Two of the 25 paired cases were wild-type across all genes. The mutational profiles, allelic imbalance status, and mutant allele frequency ratios of the paired biopsy and resection samples were highly concordant (88.75 – 98.85%), with all but three (3.7%) of the mutations identified in the resection specimens, also being present in the biopsy specimens. All 81 mutations were confirmed by QMC-PCR and HRM analysis, although four low-level mutations required a COLD-PCR protocol to enrich for the mutant alleles.

Conclusions

Diagnostic biopsies are adequate and reliable materials for molecular testing by NGS. The use of biopsies for molecular screening will enhance targeted neoadjuvant therapy.

1 INTRODUCTION

Colorectal cancer (CRC) is the third most common malignancy, and a 5th leading cause of cancer deaths worldwide [1].In the United Kingdom, CRC is the 4th most common cancer and the 5th most common cause of cancer deaths, accounting for 10% of all cancer deaths [2].Recent advances in genome sequencing technologies have enabled greater understanding of the molecular mechanisms of tumourigenesis and aided the identification of clinically relevant biomarkers for diagnosis and personalized therapeutics [3, 4].The discovery of predictive biomarkers and the development of targeted therapies are currently used in guiding personalised therapy. One example of a 'stratified medicine' approach in CRC is tumour assessment for the presence of mutations in the *KRAS or NRAS* genes, which predicts a lack of response to EGFR-targeted antibodies such as panitumumab or cetuximab [4, 5]. Constitutive activation of either *KRAS* or *NRAS* results in excess signalling through the RAS/ Mitogen-activated protein kinase pathway which cannot be negated by the anti-EGFR monoclonal antibody therapies.

Currently, tumour materials from both biopsy and resection specimens are recommended for use in the predictive testing of adjuvant targeted therapy response in stage II-III CRC, in the absence of metastatic or recurrent tumour [6]. However, the use of neoadjuvant therapy in patients with CRC is likely to increase and at present many predictive biomarkers for neoadjuvant therapy prediction are under study [7, 8]. Whilst neoadjuvant therapy is available for patients with rectal tumours, a clinical trial of neoadjuvant chemotherapy for locally advanced colonic cancer was recently started in the UK and elsewhere [7-10]. In the setting of neoadjuvant therapy, biopsy specimens may be the only available specimens to test *KRAS, NRAS* and *BRAF* mutations as recommended for the current standard-of-care of metastatic colorectal cancers. If the studies on the use of neoadjuvant therapy show desirable outcomes, then the diagnostic biopsy specimens may become the only material available for predictive testing in the neoadjuvant settings [11]. CRC develops as a consequence of waves of clonal expansion, resulting from mutations called 'driver mutations' giving a selective advantage [12]. These driver mutations, which are responsible for early clonal sweeps

through the adenoma–carcinoma sequence, should therefore be predominantly present in most of the tumour cells and consequently should be present in any biopsy samples of an individual tumour.

To confirm whether this is indeed the case and whether diagnostic biopsy specimens are appropriate for predictive testing, we have carried out mutation screening of 25 paired diagnostic biopsies (Bx) and their matched resection specimens (Rx). A sensitive next generation sequencing (NGS) approach was used to assess the presence of mutations in a panel of 26 genes involved with solid tumours.

2 MATERIALS AND METHODS

2.1 Clinical samples

FFPE sporadic CRC tumour blocks were retrieved from the archives of the Nottingham University Hospitals Department of Histopathology. All patients had undergone surgery between 2004 and 2005. Cases were selected based on the availability of clinicopathological data and the presence of at least 50% tumour cells in both Bx and Rx. DNA was extracted using the Qiagen mini Kit from 25 cases of paired biopsy samples and resection specimens as previously described [11]. Baseline characteristics are reported in Online Resource table 1.

2.2 Next generation sequencing (NGS) library preparation

Mutation profiles were determined using the TruSight tumour kit (Illumina, USA) and samples run on an Illumina MiSeq (Illumina, USA). The TruSight tumour kit offers deep coverage of 26 genes across 175 amplicons (a minimum 1000X coverage, an average of 7000X coverage). Each sample underwent a quality control (QC) step to test for template integrity according to the kit manufacturer's instructions. PCR-based library preparation was carried out in accordance with the manufacturers' instructions. The libraries were cleaned up, then diluted to a final concentration of 4nM before pooling. Captured libraries were amplified and sequenced as paired-end reads on a MiSeq flow cell, with a total of 12 samples being run on each cell.

2.3 NGS data analysis

Base calling, quality score assignment and trimming of low quality reads (using a minimum Q-score of 20) were performed on the MiSeq reporter v2.1 suite. The generated FASTQ files were aligned to the reference genome (hg19). Following alignment, the sequence variants (single nucleotide variants (SNVs) and insertions or deletions (indels)) detected in the generated BAM files were assembled into a vcf format. The Variantstudio™ v2.1analyser was used to perform variant filtering and annotation. The following criteria were used to define sequence variants -germline and somatic- and rule out mutation artefacts: (1) average wild-type read depth of >500X per

pool, (Online Resource table 2) (2) occurrence in both forward and reverse sequencing pools, (3) >3% mutant allele frequency in the merged vcf files. The dbSNP reference was used to separate germline from somatic sequence variants.

To assess the intra-assay variability of the NGS platform, we performed short-term precision assay by testing one sample in 8 replicates in the same run. The inter-assay variability was assessed with the long-term precision assay by testing the same sample in 3 different runs. For each precision assay we determined the coefficient of variation (CV).

2.4 QMC-PCR and high resolution melting (HRM) analysis

As a means of validating the mutations detected by NGS, the samples were also analysed using the quick-multiplex-consensus (QMC)-PCR in conjunction with a high resolution melting (HRM) protocol as previously described [13]. Derivative and difference plots were generated to separate mutant from wild-type samples, as described elsewhere [13, 14].

2.5 Molecular similarity between Bx and Rx

To verify if the Bx were representative of the Rx at the molecular level, we investigated the similarities between the diagnostic biopsy and resection sample pairs by using three indices which have shown relevance in the clinical and biological behaviours of cancers: *somatic mutation profiles*, *mutant allele frequency ratios* (MAFRs), and *allelic imbalance* (AI) status – within the limitations of the TruSight tumour targeted panel. Since each of the pairs of Bx and Rx are from the same tumours, they must be similar at the molecular level, i.e. not only must their mutation profiles match, but their mutant frequency ratios and allelic imbalance scores must be in the same ranges.

A crude percentage concordance was used to calculate the extent to which the diagnostic biopsies match the somatic mutation profiles, mutant allele frequency ratios, and allelic imbalance status of their corresponding resection samples, whilst the kappa test (Quick calcs (www.graphpad.com/quickcalcs/kappa2/) and Kappa (www.vassarstats.net/kappa.html)) was used to validate the crude percentage

concordance test results [15, 16]. Mean difference in MAF between Rx and Bx was calculated using the online GraphPad software (www.graphpad.com).

2.6 Performance evaluation of NGS-based somatic mutation profiling of Bx

As the 26-gene TruSight Tumour Somatic Mutation panel has translated into clinical use (www.clinicallabs.com.au/doctor/specialists-services/haematology-oncology/) we tested the following performance indices of the NGS-based somatic mutation profiling of Bx: sensitivity, specificity, negative and positive predictive values (NPV and PPV). See Online Resource table 3. The performance indices as used here are merely to show the similarities between Rx and Bx at the molecular level and not strictly as diagnostic tests of accuracy.

3 RESULTS

The NGS short-term precision assay showed a mean coefficient of variation of 12.3% (range 8.6% – 15.3%) for sequencing depth and 2.5% (range 1.6%-4.4%) for mutant allele frequency (MAF). The long-term precision assay showed a mean CV of 10.6% (range 3.2% – 15.1%) for sequencing depth and 2.2 % (range 0.01%-6.1%) for MAF. The mean sequencing depth obtained was 14803 (range 1366 – 44577), whilst the limit of detection of the mutant alleles was 3%.

3.1 Paired biopsy and resection mutation profiles

A total of 78 and 81 somatic mutations were found in the Bx and Rx samples, respectively. Only 2/25 (8%) tumour pairs displayed a wild-type genotype across all 26 genes included in the panel. The distribution of mutations detected in the 25 paired samples, are shown in table 1 and Online Resource table 2. In sample 9, the *GNAS* c.2531G>A mutation was not detected in the Bx sample. In sample 13, only the Rx contained the *GNAS* c.2543C>T mutation. In sample 20, both the Bx and Rx contained the *TP53* c.524G>A mutation, but only the Rx contained the *TP53* c.23C>T mutation. Only 8/25 (32%) of tumours contained the full complement of the *APC/KRAS(BRAF)/TP53* mutations of the Fearon and Vogelstein pathway. Furthermore, the frequency of *APC* mutations (56%) was lower than that of *TP53* mutations (68%) and this is consistent with published data. Although overall, the MAF was 1.003-fold lower in resection specimens than biopsies, but on a mutation-by-mutation basis, the MAF showed no consistent pattern of abundance between the Rx and Bx samples. Moreover, there was no significant difference in the mean MAF between Rx and Bx samples (difference in mean MAF=0.753, P=0.748). Furthermore, the three mutations not detected in Bx were present in the matched Rx at frequencies of <4%. There were no mutations in the Bx that were not seen in the Rx (table 1). In all, only 10 of the 26 genes in the TruSight panel were found to be mutated in the Rx and Bx samples.

3.2 Validation of mutations

QMC-PCR in conjunction with HRM was used to validate the mutations identified, and initially 77/81 (95.1%) of the mutations were successfully validated (Online Resource figure 1). The remaining four mutations (4.9%) were only validated by HRM following minor allele enrichment by the modified COLD-PCR protocol (Online Resource figure 2). These four "false negatives" samples were subsequently reassigned as "true positives".

3.3 Allelic Imbalance

Quantification of heterozygous SNPs was used to indicate allelic loss if there is deviation from 50% (outside the range seen in natural assay variation). Based on the maximum CV of 4.4% obtained from the short-term precision assay, and the calculated mean MAF of normal SNPs (49.9%), the normal range for SNPs in the tumour samples was calculated to be 43.3-56.5% for all SNPs. Based on this, allelic imbalance was found in Rx and matched Bx samples as shown in table 2.

3.4 Concordance in molecular alteration status between Rx and Bx pairs

To determine the similarity between Bx and their corresponding Rx at the molecular level we determined the concordance in their somatic mutation profiles. A simple 'mutation-present-or-absent' count was used to determine the mutation status match between Bx and Rx. Only the 10 mutated genes were used in this analysis which included all 50 cases (25 Bx and 25 Rx). A total of 261 Rx-Bx mutation pairs were counted (Online Resource figure 3). Of these, Bx and Rx showed concordance in 258 pairs (78 mutations and 180 no-mutations) and discordance in 3 pair (all Rx: mutations/ Bx: no-mutations). There was no Rx: no-mutation/ Bx: mutation pair. Also, all the mutations that matched were of the same bases in the same gene loci in Rx and Bx (tables 1 ~~and 3~~). A crude percentage concordance of 98.85% (258/261) was calculated for the mutation status of Rx and Bx. The event indices were input into the online kappa calculators, QuickCalcs and Kappa. The result showed a Kappa of 0.971 [standard error (SE) of 0.016 and 95% confidence interval (CI) of 0.942-1.000] which is classified as

'almost perfect' agreement (see reference 28) or 'very good' agreement (see figure 1a). Furthermore, the level of agreement between Bx and Rx in allelic imbalance status was investigated. All 25 sample pairs with 80 informative SNP loci, cumulatively, were included in the analysis. Allelic imbalance status was categorized into three classes: allelic imbalance with loss of wild-type allele (LWA, SNP % > 56.5%), allelic imbalance with loss of polymorphic allele (LPA, SNP % <43.3%) and nil allelic imbalance (NAI, SNP % within normal range of 43.3% and 56.5%). The Rx/Bx pairs were scored concordant when their SNP classes match, otherwise they were considered discordant. A total of 80 pairs were counted, comprising 51/80 NAI pairs, 7/80 LWA pairs and 13/80 LPA paired. Discordance was found between Rx and Bx in 10/80 events (Rx/Bx: NAI/LPA=3; NAI/LWA=2; LPA/NAI=2; LWA/NAI=2; LPA/LWA=0 and LWA/LPA=0) (see table 2). A crude percentage concordance of 88.75% (71/80) was calculated, giving a very good agreement between Bx and Rx for allelic imbalance status (figure 1b). Kappa test also showed a 0.76 concordance (SE of 0.076 and 95% CI between 0.612 and 0.908).

Moreover, the total MAFRs were compared between Rx and Bx. We reasoned that if Bx were truly representative of Rx's there should be some retention of the relative MAF ratios across the tumour body, despite the presence of clonal heterogeneity. A total of 20/25 sample pairs, including only Rx/Bx pairs with two or more mutations in at least one of the Rx/Bx pairs were included in this analysis. The MAFRs for both Rx and Bx were calculated relative to the MAF of the first gene loci MAF in each Rx sample on table 1. The Rx/Bx pair was considered concordant if both MAF ratios were either <1 or >1. If the MAF ratios for the Bx/Rx pair were <1 and >1, but were within 1 ± 0.05, they were also considered concordant. Otherwise, they were taken as discordant. Also, samples in which one member of the pair was missing a corresponding mutation were considered discordant and were classed into the Bx<1/ Rx>1 category as the Rx MAF ratios in all those cases were >1. A total of 58 mutation pairs were counted comprising 52 concordant observations between Rx and Bx (comprising 45 MAF ratio pairs <1, 6 MAF ratio pairs >1 and 1 MAF ratio pair $=1 \pm 0.05$) and 6 discordant observations (all Bx<1/ Rx>1). There was zero Bx:>1/Rx:<1 MAF ratio pair. A crude percentage concordance rate of 89.6% was calculated for the total MAF ratios of Rx and Bx. Kappa

was 0.651(SE=0.128, 95% CI=0.400-0.901). Both tests again returned a 'good' to 'very good' agreement scores between the MAF ratios of Bx and Rx samples (figure 1c).

3.5 Performance evaluation of NGS-based somatic mutation profiling of Bx

We evaluated the use of Bx for mutation detection by NGS using established tests of performance (Online Resource table 3). Using the Rx as the 'gold standard' samples and taking each of the somatic mutations detected (or not detected) as individual observations the following parameters were derived for Bx samples: number of true positive tests (TP)= 78, true negative (TN) =180, false positive (FP) =0 and false negative (FN) =3.

The indices of performance obtained for Bx include sensitivity of 96.3% with a false negative rate (FNR) of 3.7%, specificity of 100% with a false positive rate (FPR) of 0%, positive predictive value (PPV, precision) value of 100%, negative predictive value (NPV) of 98.4%, accuracy of 98.85%, and a false discovery rate (FDR) of 0%, altogether indicating a high performance of Bx as suitable samples for molecular testing by NGS.

4 DISCUSSION

Recent advances towards personalised medicine are driven by the identification of targetable mutations. For example, treatment of non-small cell lung cancer patients with gefitinib is dependent upon *EGFR* mutation status [18]. Herceptin administration is only considered in a subset of breast and gastric cancer patients with *HER2* amplification [18, 19]. In CRC patients with advanced disease, mutation screening of *KRAS* and *NRAS* is required prospectively, if anti-EGFR monoclonal antibody therapies are being considered, as responses have only been seen in wild-type tumours [5, 20].

Where targeted neoadjuvant chemotherapy is being offered to patients, mutation screening must be carried out on the diagnostic biopsy specimen. Thus, the question arises as to whether a biopsy specimen, which represents a tiny proportion of the tumour, is adequately representative of the whole tumour and thus can be used in patient stratification. Previously, we and others showed that FFPE diagnostic biopsy tissues were adequate for testing microsatellite instability and other molecular alterations in colorectal cancer by low throughput methods such as HRM analysis, direct sequencing, pyrosequencing, and Therascreen Amplification Refractory Mutation System (ARMS)-Scorpion [11, 21]. Furthermore, other groups have demonstrated the feasibility and reliability of the use of small diagnostic biopsies for molecular testing by NGS [22-25]. In this study, despite the use of low quality DNA template derived from FFPE tissue, we obtained a mean sequencing depth of 14803 (range 1366 – 44577) and the limit of detection for the mutant alleles was 3%. There was good short-term and long-term precision, and all 81 somatic mutations detected using the TruSight panel were also validated by QMC-PCR and HRM. Validation of low level mutations required COLD-PCR to further enrich the mutant allele population.

In our sample set, the frequency of detected gene mutations was within the range of previously published literature [26, 27]. The most frequent mutations were in *TP53* whilst *APC* mutation was found in 56% of tumours. The sensitivity of targeted NGS analysis, allowed the detection, in the biopsy samples, of all but three of the 81 mutations detected in the paired resection samples. There was no significant difference in the mean MAF between Rx and Bx samples.

More importantly, we compared the degree of similarity between the Rx and Bx pairs at the molecular level using well established statistical tests and markers which have been shown to have biological and clinical importance [5, 17, 28-33]. The presence-or-absence-of-mutation-type and the allelic imbalance status tests showed very good concordance between the Rx and the Bx samples, an indication that the latter were adequately representative of the former. Furthermore, we applied the mutant allele frequencies ratios to test the degree of similarity between the two biopsy types and found a 'good' to 'very good' concordance between them. Whilst somatic mutation profiles and allelic imbalance status have established biological, prognostic and predictive utilities, MAF is currently under active clinical research for use as a marker for the estimation of tumour heterogeneity and prediction of cancer survival, targeted therapy response and the risks and foci of tumour metastases [29-33].

Furthermore, the Bx samples showed relatively high indices of performance as potential clinical test materials for somatic mutation detection by NGS, an indication that Bx is an adequate material for molecular testing for neoadjuvant therapy.

Although, our data indicate that biopsy specimens represent a feasible material for molecular testing, but to increase the probability of sampling of the dominant clone, some factors should be considered when interpreting data from tumour biopsy specimens. For example, from where was the tissue taken? The centre, or, invasive edge of the tumour? A study performed by Baldus *et al* [34] demonstrated a discrepancy in the frequency of mutations in *KRAS*, *BRAF* and *PIK3CA* by 8%, 1% and 5% respectively between the centre and the invasive edge of colorectal tumours [34], with one explanation of this discrepancy being that the invasive edges are probably more prone to stromal contamination than the central portions of the tumour. Another factor is related to tumour clonal heterogeneity [35]. Although we did find overall a strong agreement between Rx and Bx at the molecular level, we observed that a proportion of the Rx and Bx showed MAF discrepancies at some loci and that 3/81 Bx samples did not show the corresponding mutations which were observed in the Rx samples with MAFs <4%. Based on these factors we advocate that diagnostic biopsies with intent for molecular testing should sample multiple tumour areas to enhance mutation detection.

This study is limited by the number of SNPs that could be interrogated to allow a more comprehensive AI status analysis- the TruSight panel targets gene exons

which have lower SNP densities compared to introns. Another limitation of this study is the small sample size used for the evaluation of Bx as a suitable candidate for molecular testing by NGS. The use of a larger sample size is perhaps necessary to validate the use of diagnostic biopsy as an adequate biopsy for mutation detection on the NGS platform.

In conclusion, we have shown a high concordance between matched biopsy and resection samples within the mutation distributions of the genes in the TruSight tumour panel, suggesting that the use of diagnostic biopsies is not only feasible, but also representative of the entire tumour, and thus can be used for predictive mutation screening.

Acknowledgement: The authors would like to thank Gareth Cross for enabling the process of NGS data generation and analyses.

Compliance with Ethical Standards section

This work was funded by Universities of Nottingham (for MI) and Leeds (for SDR). All the authors declare that they have no conflict of interests in publishing this manuscript. Access to tissues and ethics approval were granted by Nottingham Health Sciences Biobank, which has approval as an IRB from North West—Greater Manchester Central Research Ethics Committee (REC reference: 15/NW/0685)..

References

1. Ferlay J, Soerjomataram I, Dikshit R, Eser S, Mathers C, Rebelo M, et al. Cancer incidence and mortality worldwide: Sources, methods and major patterns in GLOBOCAN 2012. Int. J. Cancer, 2015;136: E359-E386. doi:10.1002/ijc.29210

2. Cancer Research UK (http://www.cancerresearchuk.org/health-professional/cancer-statistics/statistics-by-cancer-type/bowel-cancer/). Accessed on 20/6/2018.

3. LeBlanc VG, Marra MA. Next-Generation Sequencing Approaches in Cancer: Where Have They Brought Us and Where Will They Take Us? Farah CS, Cho WC, eds. *Cancers,* 2015; 7(3):1925-1958. doi:10.3390/cancers7030869.

4. Li J, Wang T, Zhang X, Yang X. The Contribution of Next Generation Sequencing Technologies to Epigenome Research of Stem Cell and Tumorigenesis. Human Genet Embryol, 2011; S2:001. doi: 10.4172/2161-0436.S2-001

5. Schmiegel W, Scott RJ, Dooley S, Lewis W, Meldrum CJ, Pockney P, et al. Blood-based detection of RAS mutations to guide anti-EGFR therapy incolorectal cancer patients: concordance of results from circulating tumor DNA and tissue-based RAS testing. Molecular Oncology, 2017;11(2):208-19.

6. Sepulveda AR, Hamilton SR, Allegra CJ, Grody W, Cushman-Vokoun AM, Funkhouser WK, et al. Molecular Biomarkers for the Evaluation of Colorectal Cancer: Guideline From the American Society for Clinical Pathology, College of American Pathologists, Association for Molecular Pathology, and American Society of Clinical Oncology. J Mol Diagn. 2017;19(2):187-225..

7. Santos MD, Silva C, Rocha A, Nogueira C, Castro-Poças F, Araujo A, et al. Predictive clinical model of tumor response after chemoradiation in rectal cancer. Oncotarget, 2017;8(35):58133-51.

8. Lim SH, Chua W, Henderson C, Ng W, Shin JS, Chantrill L, et al. Predictive and prognostic biomarkers for neoadjuvant chemoradiotherapy in locally advanced rectal cancer. Critical Reviews in Oncology / Hematology. 2015;96(1):67-80.

9. FoxTROT Collaboration Group. Feasibility of preoperative chemotherapy for locally advanced, operable colon cancer: the pilot phase of a randomised controlled trial. The Lancet Oncology, 2012;13(11):1152-60.

10. Jakobsen A, Andersen F, Fischer A, Jensen LH, Jørgensen JCR, Larsen O, et al. Neoadjuvant chemotherapy in locally advanced colon cancer. A phase II trial. Acta Oncologica, 2015;54(10):1747-53.

11. Fadhil W, Ibrahem S, Seth R, AbuAli G, Ragunath K, Kaye P, et al. The utility of diagnostic biopsy specimens for predictive molecular testing in colorectal cancer. Histopathology, 2012;61(6):1117-24.

12. Greaves M, Maley CC. Clonal evolution in cancer. Nature, 2012. 481(7381):306-313.

13. Fadhil W, Ibrahem S, Seth R, Ilyas M. Quick-multiplex-consensus (QMC)-PCR followed by high-resolution melting: a simple and robust method for mutation detection in formalin-fixed paraffin-embedded tissue. Journal of Clinical Pathology, 2010;63(2):134-140.

14. Seth R, Crook S, Ibrahem S, Fadhil W, Jackson D, Ilyas M. Concomitant mutations and splice variants in *KRAS*and *BRAF*demonstrate complex perturbation of the Ras/Raf signalling pathway in advanced colorectal cancer. Gut, 2009;58(9):1234-1241.

15. Quick calcs (www.graphpad.com/quickcalcs/kappa2/)

16. Kappa (www.vassarstats.net/kappa.html)

17. Nurwidya F, Takahashi F, Takahashi K. Gefitinib in the treatment of non-small cell lung cancer with activating epidermal growth factor receptor mutation. Journal of Natural Science, Biology, and Medicine, 2016;7(2):119-123. doi:10.4103/0976-9668.184695.

18. Gajria D, Chandarlapaty S. HER2-amplified breast cancer: mechanisms of trastuzumab resistance and novel targeted therapies. Expert review of anticancer therapy, 2011;11(2):263-75.

19. Abrahao-Machado LF, Scapulatempo-Neto C. HER2 testing in gastric cancer: An update. World Journal of Gastroenterology, 2016;22(19):4619-25.

20. Bokemeyer C, Cutsem EV, Rougier P, Ciardiello F, Heeger S, Schlichting M, et al. Addition of cetuximab to chemotherapy as first-line treatment for KRAS wild-type metastatic colorectal cancer: Pooled analysis of the CRYSTAL and OPUS randomised clinical trials. European Journal of Cancer, 2012;48(10):1466-75.

21. Krol LC, 't Hart NA, Methorst N, Knol AJ, Prinsen C, Boers JE. Concordance in KRAS and BRAF mutations in endoscopic biopsy samples and resection specimens of colorectal adenocarcinoma. European Journal of Cancer, 2012;48(7):1108-15.

22. Ku BM, Heo MH, Kim J-H, Cho BC, Cho EK, Min YJ, et al. Molecular Screening of Small Biopsy Samples Using Next-Generation Sequencing in Korean Patients with Advanced Non-small Cell Lung Cancer: Korean Lung Cancer Consortium (KLCC-13-01). Journal of Pathology and Translational Medicine, 2018;52(3):148-56.

23. Zheng G, Tsai H, Tseng L-H, Gocke CD, Eshleman JR, Netto G, Lin M-T. Test Feasibility of Next-Generation Sequencing Assays in Clinical Mutation Detection of Small Biopsy and Fine Needle Aspiration Specimens. Am J Clin Pathol, 2016;145:696-702.

24. Illei PB, Belchis D, Tseng L-H, Nguyen D, De Marchi F, Haley L, et al. Clinical mutational profiling of 1006 lung cancers by next generation sequencing. Oncotarget, 2017;8(57):96684-96.

25. DiBardino D, Rawson D, Saqi A, Heymann J, Pagan C, Bulman W. Next-generation sequencing of non-small cell lung cancer using a customized, targeted sequencing panel: Emphasis on small biopsy and cytology. CytoJournal, 2017;14(1):7. Available from: http://www.cytojournal.com/text.asp?2017/14/1/7/202602

26. Catalogue of Somatic Mutation in Cancer at https://cancer.sanger.ac.uk/. Accessed on 20/6/2018.

27. The Cancer Genome Atlas at https://cancergenome.nih.gov/. Accessed on 20/6/2018.

28. Viera AJ, Garrett JM. Understanding inter-observer agreement: The kappa statistic. Family Medicine, 2005 ;37(5):360-363.

29. Tejpar S, Bertagnolli M, Bosman F, Lenz H-J, Garraway L, Waldman F, Warren R, et al. Prognostic and Predictive Biomarkers in Resected Colon Cancer: Current Status and Future Perspectives for Integrating Genomics into Biomarker Discovery. The Oncologist, 2010; 15 (4): 390-404.

30. Dienstmann R, Elez E, Argiles G, et al. Analysis of mutant allele fractions in driver genes in colorectal cancer – biological and clinical insights. Molecular Oncology, 2017;11(9):1263-1272. doi:10.1002/1878-0261.12099.

31. Shen S, Wei Y, Zhang R, et al. Mutant-allele fraction heterogeneity is associated with non-small cell lung cancer patient survival. Oncology Letters, 2018;15(1):795-802. doi:10.3892/ol.2017.7428.

32. Ono A, Kenmotsu H, Watanabe M, Serizawa M, Mori K, Imai H, et al. Mutant allele frequency predicts the efficacy of EGFR-TKIs in lung adenocarcinoma harboring the L858R mutation. Annals of Oncology, 2014; 25(10):1948–1953. https://doi.org/10.1093/annonc/mdu251

33. Doma V, Papp O, Rásó E, Barbai T, Reiniger L, Vízkeleti L, Timar J. Alteration of mutant allele frequency in visceral metastases of melanoma. Journal of Clinical Oncology, 2018 36:15_suppl, e21528-e21528

34. Baldus SE, Schaefer K-L, Engers R, Hartleb D, Stoecklein NH, Gabbert HE. Prevalence and Heterogeneity of KRAS, BRAF, and PIK3CA Mutations in Primary Colorectal Adenocarcinomas and Their Corresponding Metastases. Clinical Cancer Research, 2010;16(3):790-799.

35. Yun J, Rago C, Cheong I, Pagliarini R, Angenendt P, Rajagopalan H, et al. Glucose Deprivation Contributes to the Development of *KRAS* Pathway Mutations in Tumor Cells. Science, 2009;325(5947):1555-1559.

FIGURE LEGENDS

Figure 1: Scatter plots showing the extent of agreement between Rx and Bx in the somatic mutation profile (A), allelic imbalance (AI) status (B) and mutant allele frequency (MAF) ratios (C). All the detected mutations, regardless of the MAF were included in the data that produced the somatic mutation profile and MAF ratios plots. The scatter plots show 'almost perfect' concordance in the somatic mutation profile to 'very good' and 'good' agreements in the AI status and MAF ratios, respectively.

Online Resource Figure 1: Validation of NGS-detected mutations by HRM analysis. Difference plots obtained for (A) *TP53* and (B) *KRAS*, by HRM analysis. The samples shown were identified by NGS as harbouring mutations and were confirmed by HRM analysis.

Online Resource Figure 2: HRM Analysis Difference plots showing enrichment of mutant allele by COLD-PCR. (A) A *PIK3CA* (c.331_333delAAG) mutation was detected by NGS in this sample. Plot 1 represents PCR products obtained by QMC-PCR, whilst plot 2 denotes PCR products obtained by COLD-PCR. (B) A *SMAD4* (c.1082G>A) mutation detected by NGS. Plot 1 is PCR products obtained by QMC-PCR, whereas plot 2 is PCR products obtained by COLD-PCR. * denotes baseline normal DNA.

Online Resource Figure 3: A grid chart showing the agreement status between Bx and Rx using the 'mutation-present-or-absent' test. The coloured boxes denote presence of mutations, whilst the white boxes denote absence of mutations. The coloured boxes without numbers denote that there is only one mutation type between Rx/Bx pair; the numbers in some of the boxes denote the number of mutations for each gene found in the sample pair, whilst the * denotes that the matched Bx lacked the mutation that was found in the Rx. C=concordance, D=discordance.

Figure

Click here to access/download;Figure;Figure 1_concordance graphs.jpg

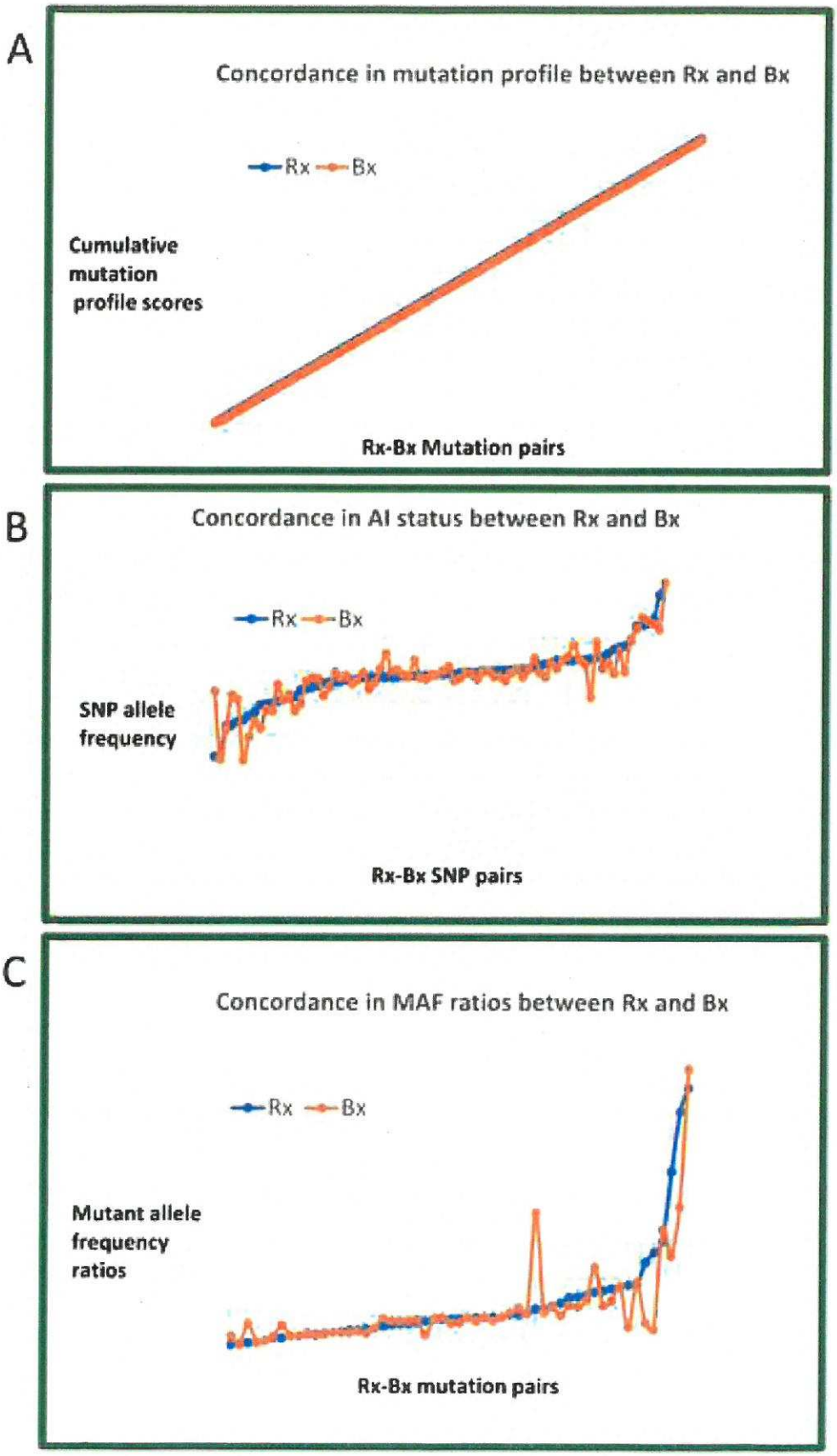

Table 1: Concordance by total mutant allele frequency (MAF) ratios

Sample No.	*Gene*	Mutation	Amino acid changes	Rx-MAF (%)	Bx-MAF (%)	Rx-MAF ratios	Bx-MAF ratios	Agreement
Rx&Bx1	*APC*	c.3997delA	Frameshift	8.96	3.94	1	1	
	APC	c.4216C>T	Q>*	11.94	4.07	1.332589286	1.032994924	C
	NRAS	c.35G>A	G>D	20.56	8.12	2.294642857	2.060913706	C
	TP53	c.273G>A	W>*	28.68	4.79	3.200892857	1.215736041	C
Rx&Bx2	*APC*	c.4216C>T	Q>*	21.99	12.96	1	1	
	KRAS	c.34G>T	G>C	33.5	22.45	1.523419736	1.732253086	C
Rx&Bx3	*APC*	c.4382_4383delAA		30.1	29.65	1	1	
	KRAS	c.35G>A	G>D	61.15	61.25	2.031561462	2.065767285	C
	TP53	c.428T>A	V>E	50.79	49.97	1.687375415	1.685328836	C
	FBXW7	c.1394G>A	R>H	32.07	30.91	1.065448505	1.042495784	C
	SMAD4	c.1609G>T	D>Y	52.87	54.63	1.756478405	1.842495784	C
Rx&Bx4	*APC*	c.4375_4376insC	Frameshift	12.91	12.09	1	1	
	KRAS	c.35G>T	G>V	35.48	33.59	2.748257165	2.778329198	C
	TP53	402_403delTT	Frameshift	45.2	45.68	3.50116189	3.778329198	C
Rx&Bx5	*TP53*	c.994-2A>C	Splice_variant	31.11	35.74	1	1	
Rx&Bx6	*APC*	c.4326delT	Frameshift	13.39	6.02	1	1	
	KRAS	c.35G>T	G>V	24.49	11.85	1.828976848	1.968438538	C
	PIK3CA	c.1633G>A	E>k	12.54	4.79	0.936519791	0.795681063	C
Rx&Bx7	*APC*	c.4732delT	Frameshift	11.66	9.56	1	1	
	KRAS	c.436G>A	A>T	11.83	9.45	1.01457976	0.988493724	C

Rx&Bx8	-	-		-	-			
Rx&Bx9	*APC*	c.4660_4661insA	Frameshift	25.1	14.91	1	1	
	KRAS	c.35G>T	G>V	29.5	15.94	1.175298805	1.069081154	C
	TP53	c.524G>A	R>H	13.53	20.14	0.539043825	1.350771294	D
	TP53	c.886C>T	R>*	3.9	3.8	0.155378486	0.254862508	C
	PIK3CA	c.331_333delAAG	Frameshift	10.23	17.37	0.407569721	1.16498994	D
	GNAS	c.2543C>T	R>H	3.38		0.134661355	0	D
Rx&Bx10	*APC*	c.3925G>T	E>*	5.53	15.2	1	1	
	APC	c.3940_3941delAG	Frameshift	6.66	16.69	1.204339964	1.098026316	C
	APC	c.3946C>T	A>V	6.83	16.96	1.235081374	1.115789474	C
	KRAS	c.38G>A	G>D	6.95	16.72	1.256781193	1.1	C
	TP53	c.623A>G	D>A	5.8	18.01	1.048824593	1.184868421	C
Rx&Bx11	*APC*	c.4216C>T	Q>*	19.94	27.48	1	1	
	KRAS	c.34G>T	G>C	18.73	24.58	0.939317954	0.894468705	C
	PIK3CA	c.290C>A	P>H	6.64	8.27	0.332998997	0.300946143	C
Rx&Bx12	*KRAS*	c.35G>A	G>D	21.99	40.36	1	1	
	TP53	c.523C>T	R>C	12.85	30.78	0.584356526	0.762636274	C
	FBXW7	c.1177C>T	R>*	12.49	27.86	0.567985448	0.690287413	C
		c.1513C>T	R>C	13.89	27.81	0.63165075	0.689048563	C
Rx&Bx13	*KRAS*	c.35G>T	G>V	10.15	4.82	1	1	
	TP53	c.186_193delAGCTC	Frameshift	7.38	4.6	0.727093596	0.954356846	C
	PIK3CA	c.247_249invTTT	Frameshift	6.59	3.77	0.649261084	0.782157676	C
	GNAS	c.2531G>A	S>F	3.05		0.300492611	0	D
Rx&Bx14	*APC*	c.4385_4386delAG	Frameshift	6.68	12.83	1	1	
	PIK3CA	c.1637A>T	Q>L	5.46	11.28	0.817365269	0.8791894	C
	FBXW7	c.1136A>T	H>L	6.05	11.74	0.905688623	0.915042868	C

	PTEN	c.801+1G>A	Splice variant	10.1	20.73	1.511976048	1.615744349	C
	SMAD4	c.1082G>A	R>H	5.47	3.4	0.818862275	0.265003897	C
Rx&Bx15	-	-		-	-			
Rx&Bx16	*BRAF*	c.1780G>A	D>N	30.69	35.29	1	1	
	TP53	c.817C>T	R>C	50.18	60.3	1.63506028	1.708699348	C
Rx&Bx17	*APC*	c.4011_4012del	LQ>L*	24.32	29.75	1	1	
	KRAS	c.38G>A	G>D	13.38	16.33	0.550164474	0.548907563	C
	TP53	c.817C>T	R>C	34.63	41.96	1.423930921	1.410420168	C
	TP53	c.874A>G	K>E	13.03	15.4	0.535773026	0.517647059	C
	PIK3CA	c.1633G>A	E>K	3.44	3.93	0.141447368	0.13210084	C
	FBXW7	c.2065C>T	R>W	44.09	38.08	1.812911184	1.28	C
Rx&Bx18	*APC*	c.4529delG	Frameshift	45.82	14.88	1	1	
	APC	c.4530C>A	S>R	46.92	15.35	1.024006984	1.031586022	C
	KRAS	c.436G>A	A>T	51.03	28.2	1.113705805	1.89516129	C
	PIK3CA	c.316G>C	G>R	16.81	22.09	0.366870362	1.484543011	D
	FBXW7	c.1513C>T	R>C	48.5	17.97	1.058489742	1.20766129	C
Rx&Bx19	*BRAF*	c.1799T>A	V>E	19.69	27.53	1	1	
	TP53	c.404G>T	C>F	28.81	48.91	1.463179279	1.776607337	C
Rx&Bx20	*TP53*	c.23C>T	P>L	3.22		1		
	TP53	c.524G>A	R>H	18.71	22.23	5.810559006	--	D
Rx&Bx21	*APC*	c.4263_4264insA	Frameshift	16.68	16.34	1	1	
	APC	c.4264_4271del	Frameshift	16.57	16.18	0.993405276	0.990208078	C
	KRAS	c.35G>T	G>V	16.97	18.25	1.017386091	1.116891065	C
	TP53	c.874A>G	K>E	51.66	52.22	3.097122302	3.195838433	C
	PIK3CA	c.1633G>A	E>K	17.7	16.36	1.061151079	1.00122399	C

	SMAD4	c.1091T>G	L>W	10.93	12.35	0.655275779	0.755813953	C
		c.1094G>A	G>D	9.95	6.98	0.596522782	0.427172583	C
Rx&Bx22	*TP53*	c.524G>A	R>H	21.52	30.03			
Rx&Bx 23	*APC*	c.2663C>T	A>V	13.63	24.05	1	1	
	APC	c.4222G>T	E>*	27.69	48.93	2.031548056	2.034511435	C
	KRAS	c.35G>A	G>D	25.38	41.69	1.862068966	1.733471933	C
	TP53	c.229C>T	P>S	51.04	47.78	3.744680851	1.986694387	C
	PIK3CA	c.325_327delGAA	Frameshift	13.75	26.56	1.008804109	1.104365904	C
	FBXW7	c.1393C>T	R>C	10.51	18.8	0.771093177	0.781704782	C
Rx&Bx24	*TP53*	c.844C>T	R>W	15.29	4.85	1	1	
	PTEN	c.795delA	Frameshift	3.15	1.85	0.206017005	0.381443299	C
Rx&Bx25	*TP53*	c.659A>G	Y>C	22.2	36.21			

***C= concordant, D=discordant**

Table 2: Allelic imbalance (AI) status of Rx and Bx

Sample pair No.	Informative SNP Loci	Rx	Bx	AI status pair	Agreement per SNP locus
1	rs2228230	45.29	48.16	NAI/NAI	C
	rs1050171	50.64	50.39	NAI/NAI	C
2	rs3733542	49.67	47.62	NAI/NAI	C
	rs41115	48.31	50.48	NAI/NAI	C
	rs1050171	71.56	61.82	LWA/LWA	C
3	rs41115	48.24	50.73	NAI/NAI	C
	rs1050171	50.62	48.36	NAI/NAI	C
	rs2023748	46.73	45.25	NAI/NAI	C
	rs41737	52.49	52.3	NAI/NAI	C
	rs1137282	26.2	24.76	LPA/LPA	C
4	rs1050171	56.24	49.35	NAI/NAI	C
	rs2023748	40.86	38.53	LPA/LPA	C
	rs41737	44.63	40.59	NAI/LPA	D
5	rs2228230	34.51	43.18	LPA/LPA	C
	rs1042522	25.62	44.24	LPA/NAI	D
6	rs41115	37.2	31.16	LPA/LPA	C
7	rs2228230	42.42	43.24	LPA/LPA	C
	rs41115	62.91	62	LWA/LWA	C
	rs2229066, rs17290559	48.83	48.74	NAI/NAI	C
	rs2023748	44.9	47.1	NAI/NAI	C

	rs41737	50.31	48.49	NAI/NAI	C
	rs1137282	40.46	39.08	LPA/LPA	C
	rs1042522	63.53	64.22	LWA/LWA	C
8	rs41115	64.73	63.53	LWA/LWA	C
	rs1137282	47.31	48.64	NAI/NAI	C
	rs1042522	53.95	58.39	NAI/LWA	D
9	rs2228230	34.4	33.38	LPA/LPA	C
10	rs3733542	50.4	49.45	NAI/NAI	C
	rs41115	50.37	47.18	NAI/NAI	C
11	rs2023748	56.85	55.89	LWA/NAI	D
	rs41737	58.6	59.13	LWA/LWA	C
	rs1042522	75.14	75.12	LWA/LWA	C
12	rs1050171	63.04	65.31	LWA/LWA	C
	rs41737	42.69	38.51	LPA/LPA	C
	rs1042522	40.24	33.67	LPA/LPA	C
13	rs41737	57.12	49.75	LWA/NAI	D
14	rs2228230	47.47	46.37	NAI/NAI	C
	rs41115	47.75	47.38	NAI/NAI	C
	rs1050171	53.44	42.62	NAI/LPA	D
	rs41737	46.97	48.12	NAI/NAI	C
15	rs3733542	48.36	48.86	NAI/NAI	C
	rs41115	54.99	52.48	NAI/NAI	C

	rs2229066, rs17290559	41.66	41.61	LPA/LPA	C
	rs2023748	49.58	49.1	NAI/NAI	C
16	rs2228230	48.77	47.72	NAI/NAI	C
	rs41115	48.42	48.31	NAI/NAI	C
17	rs2228230	48.03	49.54	NAI/NAI	C
	rs3733542	50.1	48.41	NAI/NAI	C
	rs41115	53.2	57.51	NAI/LWA	D
	rs1050171	48.24	54.96	NAI/NAI	C
18	rs2228230	48.78	49.11	NAI/NAI	C
	rs3733542	48.9	50.2	NAI/NAI	C
	rs41115	38.28	35.64	LPA/LPA	C
	rs1050171	52.07	48.21	NAI/NAI	C
	rs1137282	53.27	53.53	NAI/NAI	C
	rs1042522	51.12	53.7	NAI/NAI	C
19	rs41115	49.12	51.38	NAI/NAI	C
20	rs3733542	50.07	49.69	NAI/NAI	C
	rs41115	53.99	50.71	NAI/NAI	C
	rs1050171	35.47	41.93	LPA/LPA	C
	rs2023748	41.4	46.13	LPA/NAI	D
21	rs1050171	49.13	47.1	NAI/NAI	C
	rs35775721	48.11	44.83	NAI/NAI	C
	rs33917957	46.52	42.93	NAI/LPA	D

22	rs56391007	53.05	50.68	NAI/NAI	C
	NM_001127500.1	49.54	49.94	NAI/NAI	C
	NM_001127500.1	45.63	47.9	NAI/NAI	C
	NM_001127500.1	53.3	51.89	NAI/NAI	C
	NM_033360.2	48.23	46.66	NAI/NAI	C
	rs1042522	53.09	54.2	NAI/NAI	C
23	rs55789615	50.07	50.03	NAI/NAI	C
	rs1050171	51.67	49.47	NAI/NAI	C
24	rs3733542	49.49	48.09	NAI/NAI	C
	rs41115	36.03	24.57	LPA/LPA	C
	rs1050171	50.49	50.7	NAI/NAI	C
	rs2023748	46.86	49.58	NAI/NAI	C
	rs41737	48.55	53.15	NAI/NAI	C
25	rs41115	48.3	49.92	NAI/NAI	C
	rs1050171	48.7	48.05	NAI/NAI	C
	rs1137282	53.07	53.17	NAI/NAI	C

*C= concordant, D=discordant, I=indeterminate, NAI=nil allelic imbalance, LPA= allelic imbalance with loss of polymorphic allele, LWA= allelic imbalance with loss of wild-type allele

Online resource Figure

Click here to access/download;Figure;Online Resource Figure 1.tif

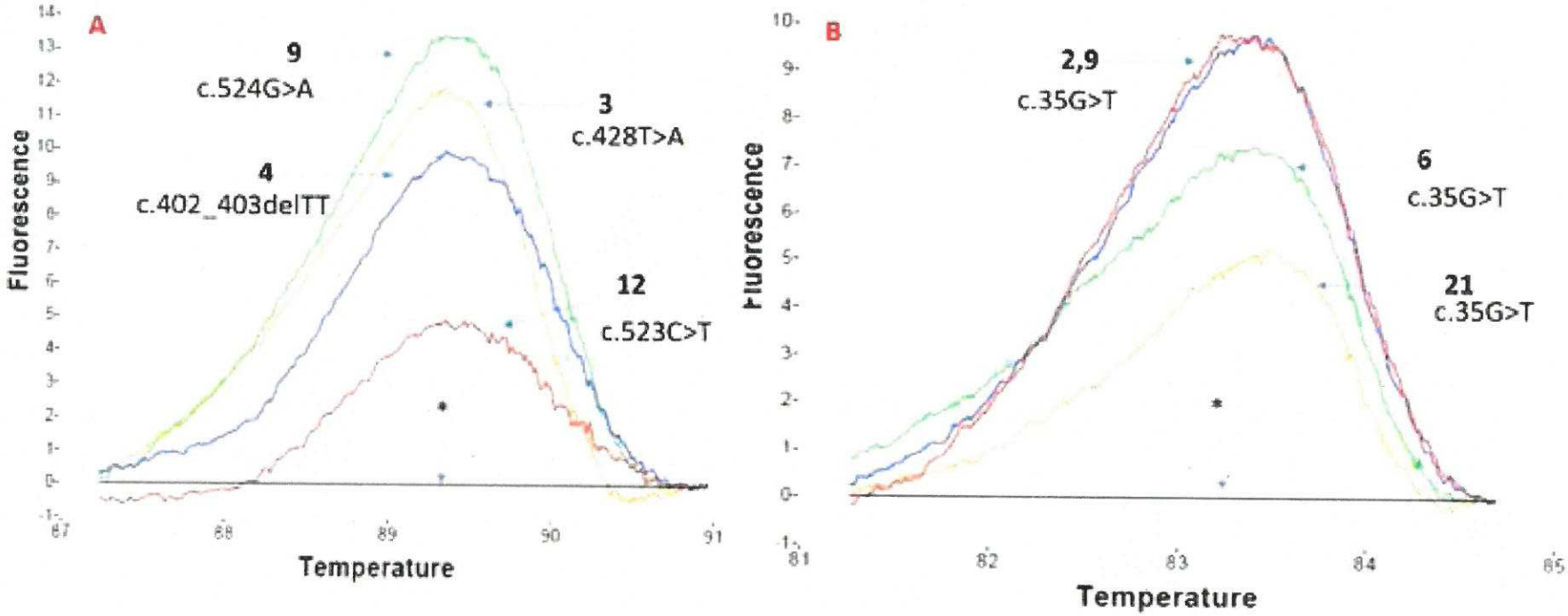

Online resource Figure

Click here to access/download;Figure;Online Resource Figure 2.tif

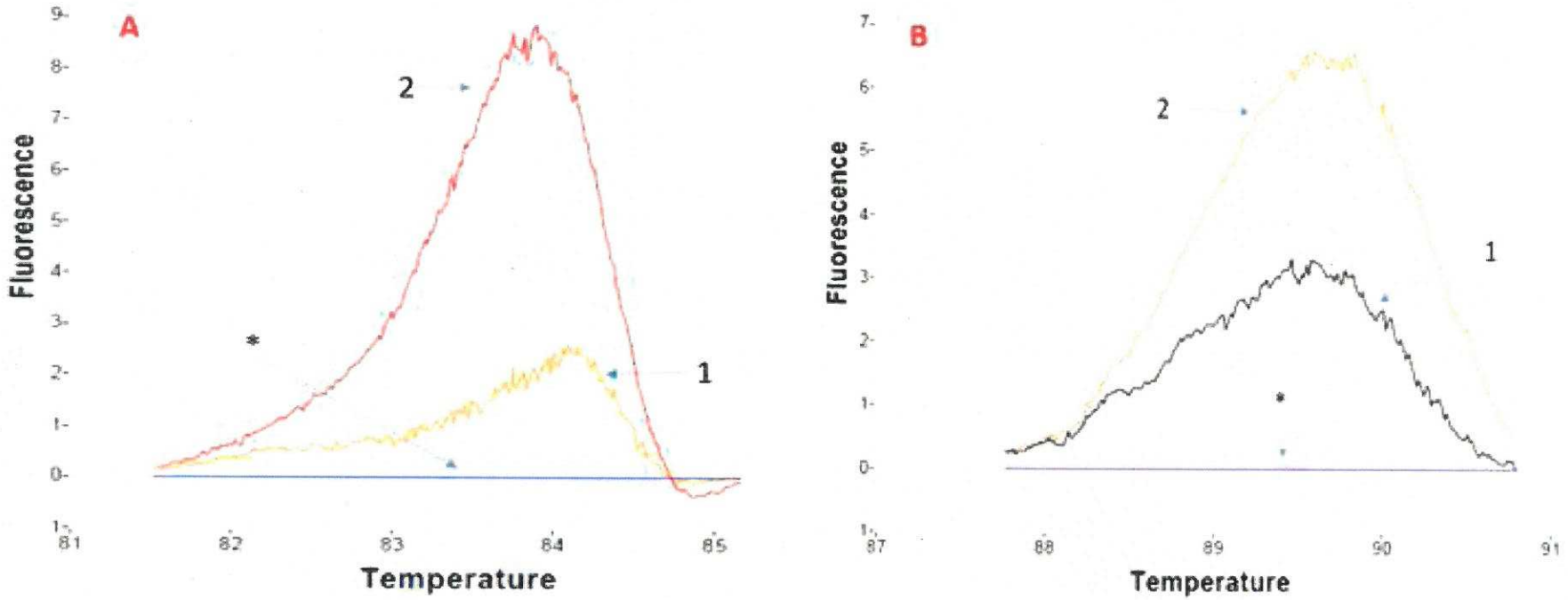

Figure

Click here to access/download;Figure;Revised Online Resource Figure 3.tif

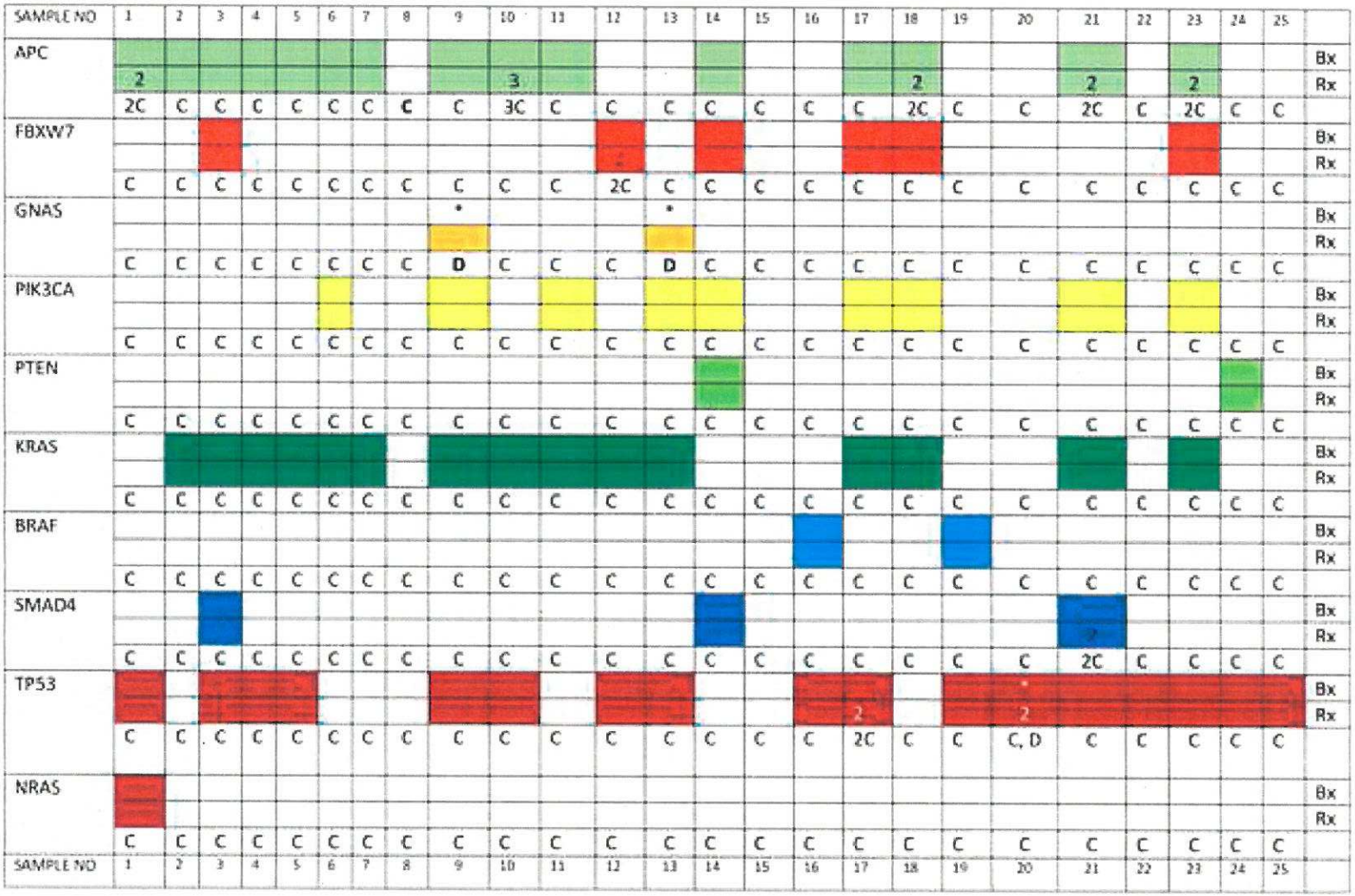

ON-LINE RESOURCE TABLES

Table 1: Clinicopathological characteristics of cases

Variable	Number %
Median age range	76 (48-87)
Gender	
Male	10 (40%)
Female	10 (40%)
Unknown	5 (20%)
Primary site	
Colon	16 (64%)
Rectum	5 (20%)
Unknown	4 (16%)
Primary T stage site	
T1	2(8%)
T2	4 (16%)
T3	13(52%)
T4	1(4%)
Unknown	5 (20%)
Primary N stage site	
N0	14(56%)
N1	3(12%)
N2	3(12%)
Unknown	5 (20%)
Tumour grade	
Moderately differentiated	16(64%)
Poorly differentiated	1 (4%)
Other	2 (8%)
Unknown	6 (24%)

Table 2: Details and frequency of all variants detected in both biopsy and resection specimens.

Case No.	Gene	Mutation	Codon	Exon	Resection			Biopsy		
					Read depth	Alt read depth	Alt variant Freq %	Read depth	Alt read depth	Alt variant Freq %
Rx&Bx1	*APC*	c.3997delA	1333	15	12904	1156	8.96	32117	1267	3.94
	APC	c.4216C>T	1406	15	25233	3014	11.94	25829	1050	4.07
	NRAS	c.35G>A	12	2	13572	2791	20.56	17257	1401	8.12
	TP53	c.273G>A	91	4	4784	1372	28.68	11000	527	4.79
Rx&Bx2	*APC*	c.4216C>T	1127	15	11971	2632	21.99	14951	1938	12.96
	KRAS	c.34G>T	12	2	10275	3442	33.5	12183	2735	22.45
Rx&Bx3	*APC*	c.4382_4383del	1461	15	6409	1929	30.1	10671	3164	29.65
	KRAS	c.35G>A	12	2	17219	10529	61.15	13894	8510	61.25
	TP53	c.428T>A	143	5	6243	3171	50.79	7578	3787	49.97
	FBXW7	c.1394G>A	465	8	27409	8791	32.07	29735	9191	30.91
	SMAD4	c.1609G>T	537	11	21170	11192	52.87	23362	12762	54.63
Rx&Bx4	*APC*	c.4375_4376ins	1459	15	17179	2218	12.91	13800	1669	12.09
	KRAS	c.35G>T	12	2	7925	2812	35.48	6180	2076	33.59
	TP53	402_403delTT	332	10	9646	4360	45.2	12112	5533	45.68
Rx&Bx5	*TP53*	c.994-2A>C	332	10	1366	425	31.11	3856	1378	35.74
Rx&Bx6	*APC*	c.4326delT	1442	15	26131	3500	13.39	11468	690	6.02
	KRAS	c.35G>T	12	2	11570	2834	24.49	6137	727	11.85
	PIK3CA	c.1633G>A	545	9	41341	5185	12.54	14994	841	4.79
Rx&Bx7	*APC*	c.4732delT	1578	15	11433	1333	11.66	9729	930	9.56
	KRAS	c.436G>A	146	4	38504	4554	11.83	31484	2974	9.45

Rx&Bx8	-	-	-	-	-	-	-	-	-	-
Rx&Bx9	*APC*	c.4660_4661ins	1554	15	35765	8978	25.1	18723	2791	14.91
	KRAS	c.35G>T	12	2	9924	2928	29.5	6392	1019	15.94
	TP53	c.524G>A	175	5	3046	412	13.53	7680	1547	20.14
		c.886C>T	196	6	1902	75	3.9	2104	81	3.8
	PIK3CA	c.331_333delAA	111	1	31127	3184	10.23	15502	2693	17.37
	GNAS	c.2543C>T	201	8	16759	566	3.38			
Rx&Bx10	*APC*	c.3925G>T	1309	15	29226	1616	5.53	28474	4277	15.2
		c.3940_3941del	1314	15	29086	1938	6.66	28154	4700	16.69
		c.3946C>T	1316	16	29202	1995	6.83	28403	4818	16.96
	KRAS	c.38G>A	13	2	7884	548	6.95	6162	1030	16.72
	TP53	c.623A>G	208	6	6652	386	5.8	5336	961	18.01
Rx&Bx11	*APC*	c.4216C>T	1406	15	31948	6371	19.94	16480	4529	27.48
	KRAS	c.34G>T	12	2	10915	2044	18.73	5866	1442	24.58
	PIK3CA	c.290C>A	97	1	18426	1223	6.64	14432	1193	8.27
Rx&Bx12	*KRAS*	c.35G>A	12	2	9296	2044	21.99	5667	2287	40.36
	TP53	c.523C>T	175	5	15627	2008	12.85	5659	1742	30.78
	FBXW7	c.1177C>T	393	9	14850	2346	12.49	7879	2195	27.86
		c.1513C>T	505	11	18781	2062	13.89	11290	3140	27.81
Rx&Bx13	*KRAS*	c.35G>T	12	2	8756	889	10.15	7205	347	4.82
	TP53	c.186_193delA	79-81	4	26264	1937	7.38	24144	1123	4.6
	PIK3CA	c.247_249invTT	83	1	8608	567	6.59	11986	452	3.77
	GNAS	c.2531G>A	205	8	17158	524	3.05			
Rx&Bx14	*APC*	c.4385_4386del	1462	15	8603	575	6.68	5907	758	12.83
	PIK3CA	c.1637A>T	546	9	29501	1611	5.46	18036	2035	11.28
	FBXW7	c.1136A>T	379	7	11711	708	6.05	11048	1297	11.74

	PTEN	c.801+1G>A	*	7	12950	1308	10.1	7763	1609	20.73
	SMAD4	c.1082G>A	361	9	13633	746	5.47	8609	293	3.4
Rx&Bx15	-	-	-	-	-	-	-	-	-	-
Rx&Bx16	*BRAF*	c.1780G>A	594	15	24432	7497	30.69	21500	7588	35.29
	TP53	c.817C>T	273	8	6144	3083	50.18	3904	2354	60.3
Rx&Bx17	*APC*	c.4011_4012del	1437-	15	20739	5044	24.32	11729	3489	29.75
	KRAS	c.38G>A	13	2	6077	813	13.38	9000	1470	16.33
	TP53	c.817C>T	273	8	6772	2345	34.63	7236	3036	41.96
		c.874A>G	292	8	3481	267	13.03	5621	365	15.4
	PIK3CA	c.1633G>A	545	9	14717	**184**	3.44	21438	843	3.93
	FBXW7	c.2065C>T	689	11	8557	3773	44.09	6326	2409	38.08
Rx&Bx18	*APC*	c.4529delG	1510	15	14781	6772	45.82	20798	3095	14.88
		c.4530C>A	1510	15	14647	6873	46.92	20477	3144	15.35
	KRAS	c.436G>A	146	4	44577	22746	51.03	31842	8980	28.2
	PIK3CA	c.316G>C	106	1	22486	3781	16.81	19929	4402	22.09
	FBXW7	c.1513C>T	505	9	19798	9603	48.5	10881	1955	17.97
Rx&Bx19	*BRAF*	c.1799T>A	600	15	35332	6958	19.69	24135	6644	27.53
	TP53	c.404G>T	135	5	6373	1836	28.81	8358	4088	48.91
Rx&Bx20	*TP53*	c.23C>T	8	2	5086	**164**	3.22			
	TP53	c.524G>A	175	5	15744	2946	18.71	10716	2382	22.23
Rx&Bx21	*APC*	c.4263_4264ins	1421	15	31777	5301	16.68	16064	2303	16.34
	APC	c.4264_4271del	1422-	15	31777	5267	16.57	16064	2278	16.18
	KRAS	c.35G>T	12	2	10231	1736	16.97	4723	862	18.25
	TP53	c.874A>G	292	8	5623	2905	51.66	4856	2536	52.22
	PIK3CA	c.1633G>A	545	9	35510	6285	17.7	14794	2421	16.36

	SMAD4	c.1091T>G	364	9	15094	1650	10.93	6080	751	12.35
		c.1094G>A	365	9	14850	1477	9.95	5963	416	6.98
Rx&Bx22	*TP53*	c.524G>A	175	5	8447	1818	21.52	15164	4553	30.03
Rx&Bx	*APC*	c.2663C>T	888	15	20303	2768	13.63	15845	3810	24.05
		c.4222G>T	1408	15	20542	5688	27.69	13631	6669	48.93
	KRAS	c.35G>A	12	2	7544	1915	25.38	7822	3261	41.69
	TP53	c.229C>T	77	4	1444	737	51.04	2030	970	47.78
	PIK3CA	c.325_327delG	109	1	25505	3506	13.75	16829	4469	26.56
	FBXW7	c.1393C>T	465	8	28121	2956	10.51	17997	3383	18.8
Rx&Bx24	*TP53*	c.844C>T	282	8	3584	548	15.29	4430	215	4.85
	PTEN	c.795delA	267	7	3924	569	14.5	4541	359	7.91
Rx&Bx25	*TP53*	c.659A>G	220	7	3379	750	22.2	5888	2132	36.21

Table 3: Performance Indices for assays

		Rx		
		Positive	Negative	Measures
Bx	Positive	TP = 78	FP = 0	PPV = 100%
	Negative	FN = 3	TN = 180	NPV = 98.4%
	Measures	Sensitivity= 96.3%	Specificity= 100%	Accuracy = 98.85%

Sensitivity= TP/(TP+FN); Specificity= TN/(TN+FP); PPV= TP/(TP+FP); NPV= TN/(TN+FN); FPR= FP/(FP+TN) = 1 – specificity; FNR= FN/(TP+FN) = 1 – sensitivity; FDR= FP/(TP+FP)